Hindawi Publishing Corporation
Journal of Wind Energy
Volume 2013, Article ID 739162, 12 pages
http://dx.doi.org/10.1155/2013/739162

Research Article

Statistical and Spectral Analysis of Wind Characteristics Relevant to Wind Energy Assessment Using Tower Measurements in Complex Terrain

Radian Belu[1,2] and Darko Koracin[2]

[1] *Drexel University, 3001 Market Street, Philadelphia, PA 19104, USA*
[2] *Desert Research Institute, 2215 Raggio Parkway, Reno, NV 89512, USA*

Correspondence should be addressed to Radian Belu; rb544@drexel.edu

Received 18 April 2013; Accepted 10 June 2013

Academic Editor: Oliver Probst

The main objective of the study was to investigate spatial and temporal characteristics of the wind speed and direction in complex terrain that are relevant to wind energy assessment and development, as well as to wind energy system operation, management, and grid integration. Wind data from five tall meteorological towers located in Western Nevada, USA, operated from August 2003 to March 2008, used in the analysis. The multiannual average wind speeds did not show significant increased trend with increasing elevation, while the turbulence intensity slowly decreased with an increase were the average wind speed. The wind speed and direction were modeled using the Weibull and the von Mises distribution functions. The correlations show a strong coherence between the wind speed and direction with slowly decreasing amplitude of the multiday periodicity with increasing lag periods. The spectral analysis shows significant annual periodicity with similar characteristics at all locations. The relatively high correlations between the towers and small range of the computed turbulence intensity indicate that wind variability is dominated by the regional synoptic processes. Knowledge and information about daily, seasonal, and annual wind periodicities are very important for wind energy resource assessment, wind power plant operation, management, and grid integration.

1. Introduction

Wind energy represents a nonpolluting, never-ending source of energy able to meet increasing energy needs domestically and around the world. Wind power is replenished daily by the sun, due to the uneven heating of the Earth's surface. Furthermore, the wind is accelerated by major land forms, so that entire regions may be very windy while others are relatively calm. A feasibility study of any wind energy project should certainly include a study of the spatial, temporal, and directional variations of wind velocity. On the other hand, the development of predictive models in order to supervise and operate wind-based electricity generation requires knowledge of the wind vector characteristics. This is a very difficult task because of the extreme transitions in the speed and direction of wind at most sites. In order to optimize wind energy conversion systems and maximize the energy extraction, annual, monthly, daily, hourly, and even by-minute frequency distributions of wind data are required. In the last few years, increasing attention has been paid to analyses of wind speed and direction statistics and to mathematical representations of wind speed and direction as being essential to wind engineering and wind energy industry. Knowledge of the wind characteristics and variability in the lower few hundred meters of the atmosphere is important to, for example, exploitation of wind energy, planning of tall buildings, and monitoring of dispersion of trace substances. For example, in the field of energy production, knowledge of the wind characteristics where wind turbine installations are planned is critical. Moreover, the development of prediction models in order to supervise and optimize the electricity generation and planning requires knowing the wind vector characteristics. An extensive review of the main issues related to the assessment and forecasting of the wind and wind energy has been shown by Koracin et al. [1]. Their review includes limitations and advantages of wind forecasting and assessment of the wind

Table 1: Names, coordinates, and elevations of the instrumented meteorological towers used in this wind energy analysis.

Site name	Lat. (deg)	Long (deg)	Alt. (m)	Distance to Tonopah 24NW Tower (km)
Luning 5N	38.57	118.18	1523	80.52
Luning 7W	38.54	118.29	1354	91.80
Tonopah 24NW	38.37	117.47	1535	0.00
Kingston 14SW	39.05	117.00	1780	85.60
Stone Cabin	38.11	116.74	2012	85.20

power density, trends of increasing penetration of wind-generated power into the utility grid, and storage of wind-generated power. They discuss the influence of wind variability, atmospheric stability, turbulence, and low-level jets on wind power density in detail. Koracin et al. [1] also reviewed prediction and assessment of climate projections of wind resources and their economic implications as well as the environmental concerns such as birds' habitats and routes, viewpoint aesthetics, and noise. The present study focuses on the cyclic evolution and the characteristics of the wind velocity fields in the complex terrain of Western Nevada using tall-tower long-term observations.

Time series of meteorological conditions are of special interest to understanding, analyzing, and modeling atmospheric phenomena, determining the climate of a geographical area, and forecasting the possibilities of occurrence of some extreme situations. Several mathematical distribution functions have been suggested to represent the wind speed, and different methods have also been developed to estimate the parameters of these distribution functions. However, the Weibull distribution is the most appropriate and most commonly used for representing the wind speed, and a great deal of work related to wind speed statistics has been reported [2–20]. Much less work has been presented in the literature regarding wind direction statistics, despite the fact that we come across directional or circular data almost everywhere in applied science. They are widely used in wind energy, biology, meteorology, geography, astronomy, air pollution, medicine, and many other areas. Data measured in the form of angles or two-dimensional orientations are unlike linear data, and they cannot be treated the same way as linear data. Wind direction, θ, is usually modeled in terms of the von Mises distribution function or in terms of a normal two-dimensional distribution function involving three parameters: the mean values of the two horizontal components of the wind speed, the RMSEs of these component values, and the correlation factors between them [13–20]. On the other hand, minimizing the fluctuations of wind energy production requires the following: (i) selecting wind farm sites having not only high wind speed but also low turbulence, (ii) optimizing the spatial distribution of the wind turbine generators within a farm by taking into account the spatial structure of the wind turbulence, and (iii) choosing the geographical distribution of the wind farms within a region or territory to favor a smoothing of the overall available wind power.

In this study, we analyze the wind speed, wind direction, diurnal, seasonal, and annual periodicities, and turbulence intensities at five sites located near Tonopah in Western Nevada (one 80 m tower and four 50 m meteorological towers; see Figure 1 for the tower locations and Table 1 for the towers' geographical coordinates). The 50 m towers were operated for a period of over four and a half years from August 2003 through March 2008, while the 80 m tower was operated from February 2007 until March 2008 [2, 21, 22]. In our analysis, we consider the wind velocity, pressure, and temperature measurements. We compare, analyze, and characterize the wind velocity characteristics and variability measured at these five instrumented tower data. The comparison and analysis are performed mainly on the basis of the aforementioned criteria. First, we characterize each measurement site by its distribution of both wind speeds and directions. The Weibull distribution function is used for the wind speed, while for wind direction the von Mises distribution function is used to draw a first comparison between these five sites [13–20]. We also analyze the periodicity characteristics of the wind speed and direction for each site. The investigation of the wind velocity for each location also permits us to highlight the influence of the site topography on the wind characteristics. A spectral characterization of the wind velocities is also presented. Finally, the analysis examines the spatial and temporal characteristics and correlations of the wind among these five instrumented towers.

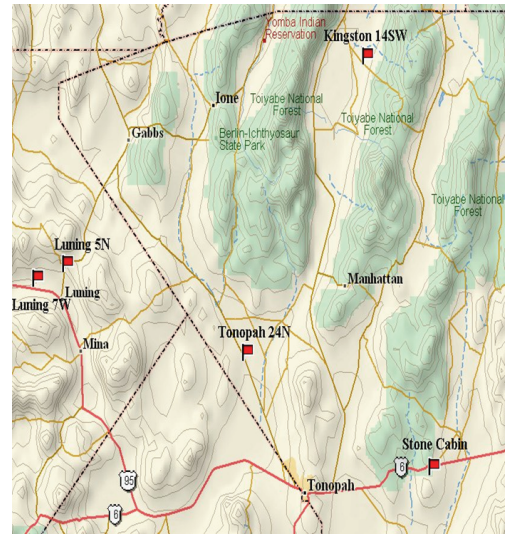

Figure 1: Topographical map showing the locations of the four 50 m towers near Tonopah, Nevada (Luning 5N, Luning 7W, Kingston 14SW, and Tonopah 24NW), and the 80 m tower (Stone Cabin).

2. Experimental Setup, Analysis Methodology, and Aspects of the Observed Wind Climate

The data analyzed in this work were collected during an experiment conducted by the Desert Research Institute near Tonopah in Western Nevada from August 2003 to March 2008 (Figure 1). The study area for the wind energy assessment conducted in this study is the complex terrain of West-Central Nevada in the proximity of the Sierra Nevada and Inyo Mountain Ranges in the Western USA. The area around the eastern slopes of the Sierra Nevada Mountains has a complex pattern of wind climate which is governed by a variety of non-linear and nonhydrostatic phenomena. A number of studies have addressed the mesoscale meteorological phenomena in this region [1, 22]. The target area for this study is located in West-Central Nevada some 100 km east of the northern tip of Inyo Mountain Range of the Sierra Nevada Mountains. Nevada is characterized by basins and mountain ranges, characterized by several mostly north-south oriented narrow mountain ranges. Secondary mountain ranges in the area reach elevations as high as 3000 m, and on average stand some as high as 1500 m over the surrounding plains. The large-scale terrain tilt is greatest towards the south. The climate is generally semiarid, and the vegetation is sparse. The aridity of the region, especially in the warmer part of the year, leads to large diurnal variations in the sensible heating. Together with the orographic features of the region, these properties are highly conducive to the onset and maintenance of thermally driven diurnal circulations. In summer, the entire region is typically characterized by deep and extremely well-mixed daytime convective boundary layers and a strong stably stratified nocturnal boundary layer with near-surface inversions [23]. On the other hand, in winter months the atmospheric processes are mainly dominated by the passages of frontal systems coming from the Pacific Ocean. The current observational evidence of the near-surface winds and their diurnal and seasonal variability in Nevada is rather poor, except for knowledge from a sparse network of surface stations and a few field experiments [1, 2, 21–23]. The experimental results suggest that, besides local thermally driven circulations, regional southwesterly plain-mountain flows driven by regional-scale heating contrasts are important components of thermally driven flows over the arid Southwest USA [1]. Some aspects of the wind speed climate related to wind power resources in this region for the aforementioned period were documented in [1, 2, 21, 22]. They showed that the strongest monthly mean wind speeds are generally found in the late afternoon, while the weakest winds are typically found in the early morning.

Wind direction θ and speed v data were measured at every 10 minutes at five levels (10 m, 20 m, 30 m, 40 m, and 50 m) at the 50 m instrumented towers. The wind speed and direction were measured in a horizontal plane, with three-cup anemometers and wind vanes (wind direction was measured only at 10 and 50 m). The accuracy of these wind measurements is 0.1 m/s for the range 5 m/s to 25 m/s. The wind velocity data collected from the 80 m tower came from sonic anemometers which were sampled at 20 Hz at four levels 10 m, 40 m, 60 m, and 80 m. Besides the wind velocity, air temperature, atmospheric pressure, humidity, and solar radiation were measured at a surface weather station located near each tower base. The goal of the experiment was to analyze and assess the wind energy potential in this area of Western Nevada. Wind velocities less than 0.5 m/s were recorded as calm and were not included in this analysis. Before the statistical and spectral analysis of the data, a quality control check of all data was performed to remove outliers and to interpolate over small data gaps that may be present. Overall, the corrected data are of sufficient quality, with less than 3% of the data removed as outliers or unacceptable data [2, 22].

3. Data Analysis and Results

Assessment of the wind energy potential at a particular site or area involves analyzing the wind characteristics, the distribution of the measured wind speed and direction, the maximum wind speed, the wind variability and seasonality, and the diurnal variations of the wind speeds. Wind characteristics were studied by using cumulative frequencies of the observed wind velocities and the Weibull and the von Mises probability distributions. To understand the diurnal, seasonal, and annual variations of the wind speeds and direction, a comprehensive statistical and spectral analysis was performed.

3.1. Wind Speed and Wind Direction Distributions. First, we performed a meteorological analysis of the composite 2003–2008 50 m tower datasets for the four 50 m meteorological towers and of the 14-month data measured at the 80 m tower. We analyzed the measured wind and meteorological data using statistical descriptors (mean and variance) and the relative and cumulative frequencies at each tower and measurement level. The air density was calculated using pressure and temperature measurements. The monthly and annual averages of the wind speed, temperature, pressure, and air density are summarized in Table 2. Due to location elevations, the monthly values of the air density at each of the five sites range from 0.950 to 1.100 kg/m^3, which are significantly lower than those the standard air density of 1.225 kg/m^3. The Tonopah 24NW and Stone Cabin sites show higher monthly wind speeds compared with the other towers. Monthly wind speeds at the 30 m level of the Luning 7W Tower are higher than the values measured at the 50 m level. Similarly, the wind speeds at 60 m for Stone Cabin are in general higher than those at the 80 m level. This pattern is very likely due to the effects of the local complex topography on the air flows. The towers are located in complex terrain with a complex wind climate. The dominant directions (at the 10 m and 50 m levels) for the wind at Tonopah 24NW are north-northwest and south, while for Kingston 14SW they are north-northeast and south-southwest. The Kingston 14SW Tower is located on a high plain to the east of a mountain ridge oriented almost north-south. The dominant directions for the Stone Cabin Tower are equally divided between northwest and southwest. For Luning 7W, the dominant directions

Table 2: Monthly average wind speed and air density based on 2003 to 2008 composite datasets for the 50 m towers and February 2007 to March 2008 Stone Cabin Tower data.

Tower parameter	Jan.	Feb.	Mar.	Apr.	May.	Jun.	Jul.	Aug.	Sep.	Oct.	Nov.	Dec.	Annual average
Tonopah 24NW													
V_{mn} (m/s), 50 m	4.97	5.44	5.85	6.52	6.22	6.35	5.25	5.08	5.30	5.41	5.04	4.53	5.49
V_{mn} (m/s), 30 m	4.69	5.09	5.50	6.13	5.83	5.94	4.90	4.79	5.01	5.12	4.79	4.33	5.17
V_{mn} (m/s), 10 m	4.33	4.73	5.11	5.73	5.45	5.56	4.62	4.48	4.69	4.75	4.43	4.04	4.82
ρ (kg/m^3)	1.084	1.071	1.053	1.038	1.016	0.997	0.985	0.994	1.015	1.039	1.081	1.086	1.036
Kingston 14SW													
V_{mn} (m/s), 50 m	3.73	4.21	4.81	5.51	4.93	5.27	4.69	4.66	4.35	4.22	3.45	3.99	4.53
V_{mn} (m/s), 30 m	3.25	3.71	4.30	4.95	4.44	4.78	4.26	4.11	3.80	3.64	2.98	3.48	4.01
V_{mn} (m/s), 10 m	2.81	3.20	3.81	4.34	3.94	4.22	3.80	3.69	3.44	3.29	2.70	3.06	3.56
ρ (kg/m^3)	1.059	1.045	1.029	1.015	0.995	0.977	0.964	0.972	0.992	1.015	1.013	1.058	1.055
Luning 7W													
V_{mn} (m/s), 50 m	3.74	4.14	3.68	4.30	4.48	4.45	3.81	3.32	3.51	3.94	3.69	4.75	3.96
V_{mn} (m/s), 30 m	4.02	4.12	4.09	4.53	4.33	4.23	3.66	3.52	3.59	4.01	3.80	4.68	4.03
V_{mn} (m/s), 10 m	3.51	3.63	3.69	4.03	3.82	3.73	3.21	3.13	3.20	3.48	3.27	4.00	3.54
ρ (kg/m^3)	1.108	1.092	1.072	1.057	1.033	1.015	1.000	1.010	1.032	1.067	1.093	1.105	1.055
Luning 5N													
V_{mn} (m/s), 50 m	3.11	3.77	4.14	4.63	4.50	4.40	3.69	3.51	3.41	3.63	3.26	3.81	3.81
V_{mn} (m/s), 30 m	2.80	3.46	3.83	4.33	4.20	4.10	3.42	3.24	3.15	3.25	2.91	3.43	3.49
V_{mn} (m/s), 10 m	2.52	3.00	3.48	3.88	3.73	3.60	2.99	2.06	2.86	2.90	2.70	3.05	3.12
ρ (kg/m^3)	1.080	1.067	1.048	1.036	1.015	1.000	0.983	0.991	1.011	1.043	1.068	1.079	1.033
Stone Cabin													
V_{mn} (m/s), 80 m	5.123	5.562	5.525	5.752	5.883	5.667	5.061	3.985	4.514	6.463	4.536	4.988	5.255
V_{mn} (m/s), 60 m	6.034	6.243	5.945	6.125	6.287	5.955	5.461	3.935	5.208	6.757	4.542	5.619	5.676
V_{mn} (m/s), 40 m	5.652	5.908	5.661	5.751	5.883	5.673	5.163	3.793	4.683	6.255	4.197	5.352	5.445
V_{mn} (m/s), 10 m	4.460	4.875	4.588	4.717	4.918	4.338	3.919	2.517	3.004	4.468	3.236	4.201	4.104
ρ (kg/m^3)	0.982	0.962	0.945	0.936	0.941	0.962	0.984	0.997	1.025	1.025	1.014	1.008	0.982

of the wind are eastwest, while for Luning 5N they are north-northwest and south-southeast. The shift of about 60° in the wind directions for the Luning 7W Tower compared with the Luning 5N Tower (the towers are in proximity of each other, about 10 km distant, but with about 170 m elevation difference; see Table 1 for the tower altitudes and coordinates and Figure 1) is accounted for by the effects of the local topography and maybe the effect of the difference in the altitude on flow patterns. These two towers are in proximity of a small mountain ridge with an eastwest orientation.

The multiannual monthly means of wind speed and direction are in very good agreement with the climatologic values for Nevada found in the literature [1, 22–24]. The Tonopah 24NW site seems to be the most promising wind energy site of all four towers (with seasonal means from 5.25 to 6.20 m/s and with a multiannual value of 5.49 m/s, class 3 or higher wind power potential), at the 50 m level. The Kingston 14SW site has seasonal mean values between 3.97 m/s and 5.08 m/s and a multiannual value of 4.53 m/s, class 2 or higher wind power potential. For the other two towers, the seasonal mean values are around 4 m/s or lower, class 1 wind power potential [25]. The Stone Cabin Tower at the 60 m level has seasonal mean values between 5.12 m/s and 6.12 m/s and an annual value of 5.68 m/s, the same wind class potential as that of the Tonopah 24NW site. For the other levels, these values are smaller. The Stone Cabin site seems to be in the same wind energy potential class as that of the Tonopah 24NW site, although this site has a much shorter period of observations, only 14 months. Note that the monthly multiannual wind speeds for the Tonopah 24NW and Stone Cabin Towers are in the range of 6.5 m/s to 7.5 m/s (wind class 4) during the peak season (February to June) and 5.5 m/s to 6.5 m/s (wind class 3) for the rest of the year. For the Kingston 14SW 50 m Tower, the wind speeds are in the range 4.7 m/s to 5.8 m/s during the peak season (wind class 2) and between 3.7 m/s and 4.3 m/s for the rest of the year. The other two 50 m towers are showing slightly lower wind potential than that of the Kingston 14SW site. Table 2 summarizes the statistical data for all towers and data sets.

Monthly values are for the 2003–2008 composite datasets for the 50 m towers and for 2007-2008 for the 80 m towers. The use of probability distribution functions to define, characterize, and fit the field data has a long history. It is established that the Weibull distribution [2–20, 26] can be used to characterize wind speed regimes in terms of its probability density and cumulative distribution functions, and it is commonly used to estimate and to assess wind energy potential. Although efforts were made over the years to fit measured wind data to other distributions such as exponential distribution, Pearson' type VI distribution, logistic distribution,

Table 3: The Weibull parameters and wind characteristics derived from the Weibull distribution. Monthly values are for the 2003–2008 composite datasets for the 50 m towers and for 2007-2008 for the 80 m tower.

Tower (50 m level) parameter	Jan.	Feb.	Mar.	Apr.	May.	Jun.	Jul.	Aug.	Sep.	Oct.	Nov.	Dec.	Annual average
Tonopah 24NW													
k (-)	1.505	1.630	1.730	1.748	1.919	1.939	1.924	1.932	1.830	1.721	1.600	1.487	1.703
c (m/s)	5.389	5.977	6.431	7.221	6.881	7.017	5.764	5.569	5.810	6.007	5.537	4.953	6.041
V_{mn} (m/s)	4.86	5.35	5.73	6.43	6.10	6.22	5.11	4.94	5.16	5.36	4.96	4.48	5.39
Kingston 14SW													
k (-)	1.231	1.404	1.474	1.588	1.631	1.654	1.610	1.583	1.481	1.403	1.280	1.211	1.415
c (m/s)	3.913	4.519	5.182	5.988	5.350	5.754	5.103	4.994	4.698	4.506	3.973	4.228	4.821
V_{mn} (m/s)	3.66	4.12	4.69	5.37	4.79	5.14	4.57	4.48	4.25	4.11	3.68	3.97	4.39
Luning 7W													
k (-)	1.248	1.361	1.182	1.298	1.475	1.506	1.550	1.365	1.315	1.304	1.297	1.409	1.346
c (m/s)	4.353	4.609	4.120	4.853	4.855	4.854	4.177	3.737	3.803	4.303	4.095	5.256	4.385
V_{mn} (m/s)	4.06	4.22	3.97	4.48	4.39	4.38	3.76	3.42	3.51	3.98	3.78	4.79	4.02
Luning 5N													
k (-)	1.229	1.278	1.274	1.347	1.410	1.397	1.445	1.406	1.278	1.236	1.236	1.195	1.335
c (m/s)	3.166	3.945	4.306	4.900	4.746	4.668	3.958	3.672	3.552	3.736	3.348	3.949	3.992
V_{mn} (m/s)	2.96	3.66	3.99	4.50	4.32	4.26	3.59	3.35	3.29	3.49	3.13	3.72	3.67
Stone Cabin (60 m level)													
k (-)	1.369	1.271	1.877	1.814	2.298	1.990	2.049	2.041	1.956	1.897	1.996	1.273	1.812
c (m/s)	7.386	5.451	4.822	5.527	4.847	4.969	4.916	4.861	5.125	4.849	3.345	5.981	5.177
V_{mn} (m/s)	7.39	5.45	4.83	5.53	4.85	4.97	4.92	4.86	5.13	4.85	3.35	5.98	5.29

and so forth, the Weibull distribution is well accepted and widely used for wind data analysis. The probability density function of a Weibull distribution (f_{WB}) is given by

$$f_{WB} = \frac{k}{c}\left(\frac{v}{c}\right)^{k-1} \exp\left(-\left(\frac{v}{c}\right)^{k}\right). \quad (1)$$

The factors k and c featured in (1) are the shape and the scale parameters, respectively, which are determined for each measurement site. The function $f_{WB}(v)$ is the probability of observing the particular wind speed, v. There are several estimators of the Weibull parameters [3–8, 24], such as the Moment, Maximum Likelihood, Least-Square, and Percentile Estimators methods. These estimators are unbiased, although some of them, such as the method of Moments, may have large variances, so there is no reason to prefer any of them. We selected three estimators of the Weibull parameters: the standard least-square, the maximum likelihood, and a variation of the maximum likelihood methods. The shape and scale parameters are determined by taking the averages of the estimates found by these methods. Table 3 gives the monthly and annual values of the shape (k) and scale (c) parameters of the wind speed distribution for all towers computed for the composite datasets. As with the mean monthly wind speed, the monthly scale parameter values are higher during the peak season than for the rest of the year for all towers and levels of observations. Figure 2 shows the wind speed data distributions for the Tonopah 24NW and Kingston 14SW towers at the 50 m height level and for the Stone Cabin Tower at the 60 m level. The fitted Weibull probability distributions are in good agreement with our experimental data for all towers. For the multiannual Weibull distributions, the mean root-mean-square error (RMSE) and the Chi-square χ^2 values are about 0.02 and 0.01, respectively.

The wind rose diagrams and wind direction frequency histograms provide useful information on the prevailing wind direction and availability of directional wind speed in different wind speed bins. The wind roses were constructed using the composite datasets of measurements of wind velocities, and they are shown in Figure 3 for the 50 m height level for the Tonopah 24NW, Kingston 14SW, and Stone Cabin Towers, respectively.

The wind direction was analyzed using a continuous variable probability model to represent distributions of directional wind speeds. The model is comprised of a finite mixture of the von Mises distributions (vM-PDFs), following the approaches given in [17, 18, 27]. The parameters of the models are estimated using the least-square method [17, 18]. The range of integration to compute the mean angle and standard deviation of the wind direction is adjusted to minimum variance requirements. The suitability of the distribution is judged from the mean-square error (MSE), found to be around 10% or lower. The proposed probability model $mvM(\theta)$ is comprised of a sum of N von Mises probability density functions, $vM_j(\theta)$, as

$$mvM(\theta) = \sum_{j=1}^{N} w_j vM_j(\theta), \quad (2)$$

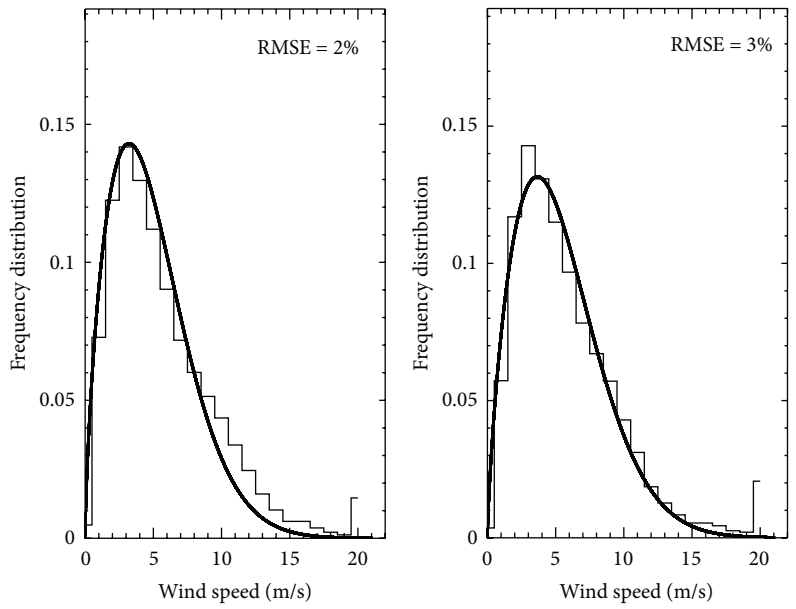

Figure 2: Wind speed frequency distributions for the Tonopah 24NW Tower (a) at 50 m, for 2003–2008 composite datasets, and the Stone Cabin Tower (b) at 60 m for 2007-2008 composite dataset.

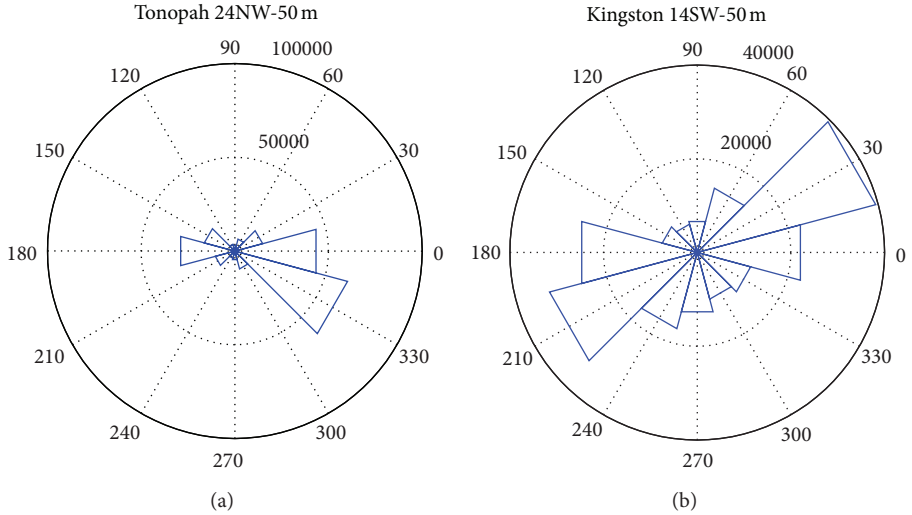

Figure 3: Wind rose diagrams for the composite 2003–2008 datasets at 50 m for the Tonopah 24NW Tower (a) and the Kingston 14SW Tower (b).

where w_j are nonnegative weighting factors that sum to one [17]:

$$0 \le w_j \le 1 \quad \left(j = 1, \ldots, N, \sum_{j=1}^{N} w_j = 1 \right). \tag{3}$$

A random variable function has a von Mises distribution *vM-PDFs* if its probability is defined by the folowing equation:

$$vM_j\left(\theta; k_j, \mu_j\right) = \frac{1}{2\pi I_0\left(k_j\right)} \exp\left[k_j \cos\left(\theta - \mu_j\right)\right], \quad 0 \le \theta \le 2\pi, \tag{4}$$

where $k_j \ge 0$ and $0 \le \mu_j \le 2\pi$ are the concentration and mean direction parameters, respectively. In this paper, the wind direction is where the wind is coming from, while the angle corresponding to the northerly direction is taken as 0°. Note that, in meteorology, the angle is measured clockwise from the north. Here, $I_0(k_j)$ is a modified Bessel function of the first kind and zero order and is given by

$$I_0\left(k_j\right) = \frac{1}{2\sqrt{\pi}} \int_0^{2\pi} \exp\left[k_j \cos\theta\right] d\theta \approx \sum_{p=0}^{\infty} \frac{1}{\left(p!\right)^2} \left(\frac{k_j}{2}\right)^{2p}. \tag{5}$$

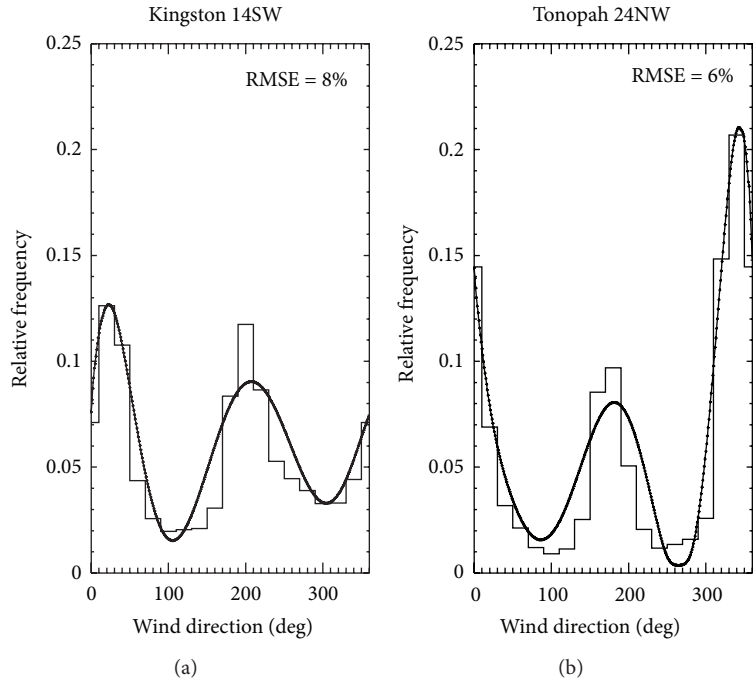

Figure 4: Frequency histograms of wind directions and the fitted von Mises distribution functions at the Tonopah 24NW Tower (a) and the Kingston 14SW Tower (b) at 50 m using the composite 2003–2008 datasets.

The distribution law $mvM(\theta)$, given by (2), can be numerically integrated between two given values of θ to obtain the probability that the wind direction is found within a particular angle sector. Various methods are employed to compute the 3 N parameters on which the mixture of the von Mises distribution depends [14–17]. In this paper, we follow the approach presented in [18], employing the least-square (LS) method. In this method, the 3 N unknown values of the parameters, μ_j, k_j, and w_j, are estimated by minimizing the sum of squares of the deviations between the experimental and model data under linear inequality constraints. The full description of this method can be found in [18, 19] or elsewhere in the literature. We can also note that the presence of calm winds in the wind data (wind speeds less than or equal to 0.5 m/s) leads to the appearance of gaps in the speed and direction data series, which makes the calculation of the statistical properties of the directional wind speed biased. These values are excluded from our computation of wind direction statistics. Figure 4 shows the wind direction frequency histograms for the Kingston 14SW and Tonopah 24NW Towers using the composite 2003–2008 datasets and Stone Cabin tower using the 2007-2008 composite dataset. The fitted the von Mises distributions are also shown on these graphs. The number of components (2) of the composite von Mises distribution for these two datasets was $N = 2$, while the mean-square errors between the measurements and the fitted distributions are in the range of 10% or lower. Similar results were found for all other towers used in this analysis.

Turbulence intensity (TI), defined as the ratio of the standard deviation over the wind speed, is an indicator of turbulence and not an absolute value, a very useful indicator in wind turbine operation and design. Notice that the maximum distance between the 50 m towers is about 200 km. Each site is situated in a complex terrain area, but we expect to see similar synoptic wind conditions. However, the comparative analysis of the values in Table 4 shows that even on large time scales (the four and half years period) the wind characteristics are influenced by the location. Table 4 also gives us the two following coefficients of variation, defined as:

$$\overline{\mathrm{TI}} = \left(\frac{1}{N}\right)\sum_{i=1}^{N}\left(\frac{\sigma_i}{v_i}\right), \tag{6}$$

where σ is the standard deviation of the wind speed computed at each site, using the composite 2003–2008 datasets of measurements and thus including time scales ranging from ten minutes up to fifty-four months. The symbols σ_i and v_i stand for the time-specific interval-averaged values of the wind speed standard deviation and the wind speed. The coefficient of variation corresponding to time scales larger than ten minutes is $\overline{\mathrm{TI}}_{T>10}$, while $\overline{\mathrm{TI}}_{T<10}$ is the mean coefficient of variation for time scales smaller than ten minutes. Unlike the mean wind speed which is influenced by the location, these coefficients of variation remain rather similar for all five sites. The values given in Tables 3, 4, and 5 are sufficient for a first rough estimation of the mean wind power production of each site. However, for the sake of complete wind energy potential assessment, wind energy conversion operation, or grid integration, some supplementary information is needed concerning periodicity and more generally time variability of the wind velocity for a given time scale. In the next two subsections of this paper, a comprehensive analysis of the wind velocity variability and periodicities will be performed.

Table 4: Overall wind speed and direction characteristics, turbulence intensity, and coefficient of variations for the wind speed for time scales larger than one month.

Tower	Mean wind speed (m/s)	Mean wind direction	σ (m/s)	$\overline{\mathrm{TI}}_{T<10}$	$\overline{\mathrm{TI}}_{T>10}$	k	c
Kingston 14SW	4.48	162	3.37	0.20	0.75	1.415	4.82
Tonopah 24NW	5.49	223	3.41	0.17	0.62	1.703	6.04
Luning 7W	3.96	191	3.06	0.25	0.77	1.346	4.39
Luning 5N	3.77	185	3.03	0.25	0.80	1.335	3.99
Stone Cabin (60 m)	5.24	165	3.66	0.18	0.66	1.667	5.92

Table 5: Coefficient of variations for the wind speed for time scales larger than one month.

Tower	Coefficient of variation $\mathrm{TI}_{T>1\,\mathrm{month}}$
Kingston 14SW	0.30
Tonopah 24NW	0.26
Luning 7W	0.36
Luning 5N	0.35
Stone Cabin (60 m)	0.27

3.2. Wind Speed Seasonality and Variability for Time Scales Larger Than One Month. To put in evidence the dynamical behavior of the wind speed for time scales larger than one month, a low-pass filter was applied to the measured wind speed signal. We use here the simplest one, that is, the moving average calculation:

$$\overline{U_N}(k) = \sum_{i=k-(N-1)/2}^{i=k+(N-1)/2} v_i. \tag{7}$$

The moving averages corresponding to an averaging period of one month computed using the wind speed measured at each site, for the 10 m, 30 m, and 50 m levels, at the Tonopah 24NW tower are shown in Figure 5. Figure 6 shows the moving averages for all 50 m towers, for the composite 2003–2008 datasets. These plots give a first indication of the seasonal variations of the wind speed over the five sites and seem to indicate a typical annual cycle, with a maximum during spring and with a minimum during fall. It is clear that a longer measurement period is required to further confirm the seasonality in Figures 5 and 6. Another result is the fairly good similarity of the variations of the large time scales for the four 50 m towers. This is confirmed by the cross-correlation coefficients between the four sites. The cross-correlation coefficient is defined by

$$R_{xy}(\tau) = \begin{cases} \sum_{k=0}^{N-\tau-1} \dfrac{x_{k+\tau} y_k}{\sigma_x \sigma_y} & \tau > 0, \\ R_{xy}(\tau), & \tau < 0, \end{cases} \tag{8}$$

where x and y are zero-mean stochastic variables and σ_x and σ_y are their standard deviations.

The computed values of the cross-correlation coefficients of the four 50 m towers for smaller time lags are around 0.6, showing quite similar wind climatology, for this area. This is another very strong indication of the stability and uniformity

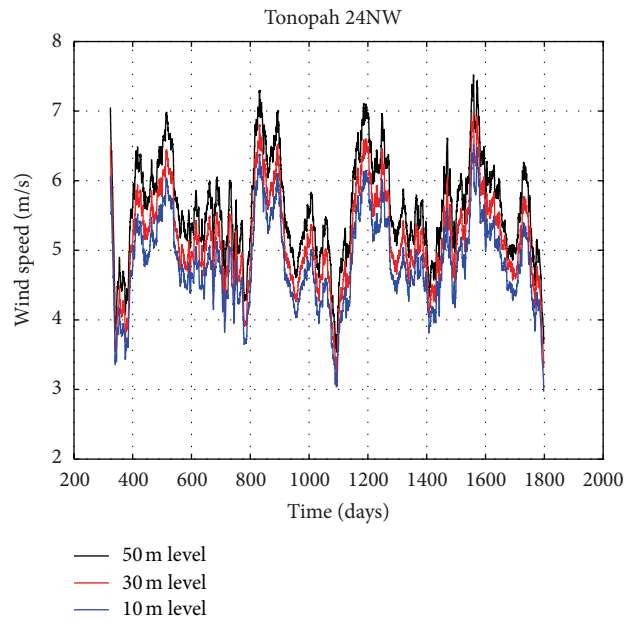

Figure 5: Moving average time series of the wind speed for the Tonopah 245NW Tower, at 50 m, 30 m, and 10 m levels, and for the composite 2003–2008 datasets.

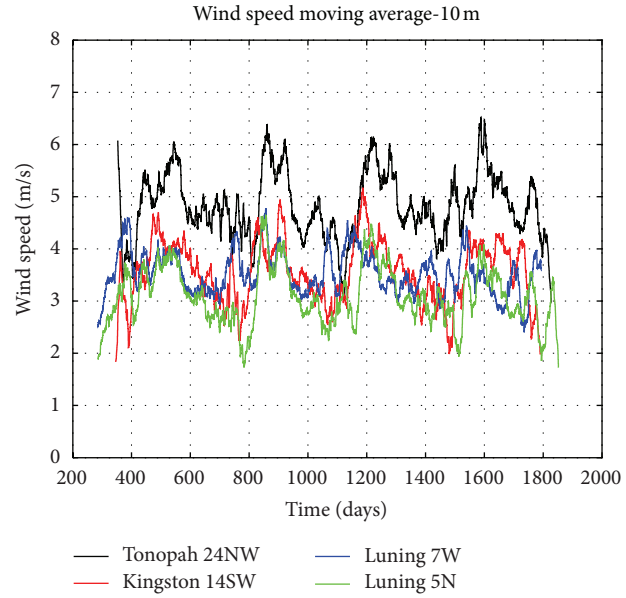

Figure 6: Wind speed moving average for the four 50 m towers; the averaging time is equal to 4032 hours (4 weeks), and at 10 m level.

of the wind characteristics in Western Nevada. This is a very important characteristic for wind energy assessment, as well as wind power plant operation, management, and grid integration. The coefficient of variation over time scales larger than one month is given by

$$\mathrm{TI}_{T>1\,\mathrm{month}} = \frac{\sigma_{T>1\,\mathrm{month}}}{\overline{U}}, \tag{9}$$

where $\sigma_{T>1\,\mathrm{month}}$ is the standard deviation for wind variations for time scales larger than one month. Table 5 gives $\mathrm{TI}_{T>1\,\mathrm{month}}$ for each of the four 50 m towers and for the 2003–2008 composite datasets. These coefficients of variations are found to be rather similar. This is a consequence of the similarity of the wind characteristics and the uniformity of the wind variability of this region of Nevada [1–3, 21–24]. For a statistical analysis of wind data, we computed autocorrelation and cross-correlation functions of the wind speeds and wind directions (with the longest lag of 28 days), for all towers and for all levels of measurements. Using a similar relationship as in (9), where the y is replaced by x, the autocorrelation coefficients can be computed.

Figure 7 shows the autocorrelation functions of the wind speed, at the 50 m, for all of the four 50 m towers analyzed. It can be observed that all of these functions are coincidental and are showing similar periodicity. A similar pattern in the autocorrelation functions was found for the Stone Cabin Tower at all levels, even for the shorter dataset. Regular oscillations exist, indicating that a quite well-defined periodicity characterizes the wind speed in Western Nevada. A very slow decrease in the amplitude of the oscillation as the lag time τ increases indicates that the wind speed is not strictly periodic, but it is randomly modulated in frequency and phase. This behavior is also observed in the wind direction autocorrelation functions illustrated in Figure 8. The maintained oscillatory character of these functions indicates that the dominant frequencies associated with the wind speeds and directions are roughly coincidental. Similar patterns were found for all levels and towers, both for autocorrelations of wind speed or wind direction and for cross-correlations of wind speed and directions. This fact indicates that the wind speed and wind direction signals are in phase. It can be also noted that the lag times corresponding to the maximum values of the autocorrelation functions are about 24 hours. This period of 24 hours, as the dominant of the signals, shows that this is the time interval that basically governs the changes in wind speed and wind direction. This fact is related to the different behavior of the day and night winds which roughly maintain their structure during almost the five years of the time interval analyzed.

Two facts are immediately apparent in all of the autocorrelation data analyzed. First, the presence of a strong sinusoidal component at diurnal frequency which is almost constant as the lag value increases indicates that it is derived from a deterministic period component. The second feature is that the centerline of the diurnal component is not the zero datum line, but it is offset above the lag axis. This offset cannot be due to a zero mean (which is removed by the autocorrelation algorithm), suggesting the presence of another periodic component of a much lower frequency.

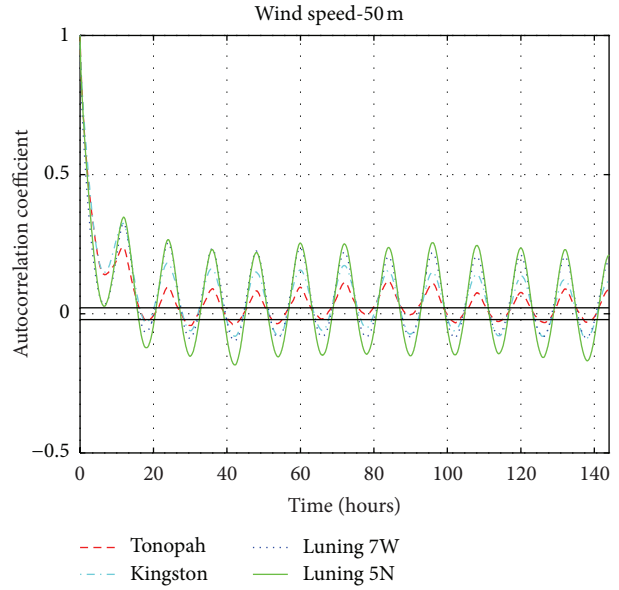

Figure 7: Autocorrelation functions for 10 min wind speed, for all 50 m towers, and for 50 m level; the 2003–2008 composite datasets, with 95% confidence intervals, are also shown on the graph.

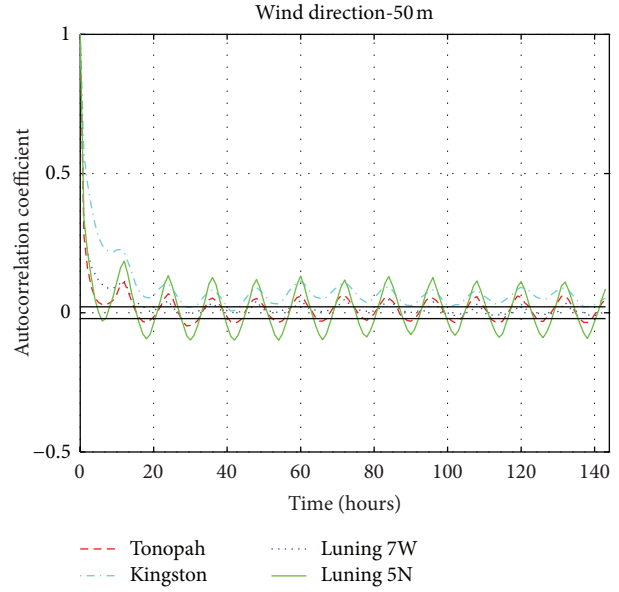

Figure 8: Autocorrelation of 10 min wind direction, for all 50 m towers and for 50 m level; the 2003–2008 composite datasets, with 95% confidence intervals, are also shown on the graph.

The obvious candidate for investigation was an annual cycle. This is also in agreement with the presence of a spring maximum and a fall minimum in the wind speed moving average time series (Figures 5 and 6). In order to investigate the possible presence of an annual cycle, daily mean data for the whole period August 2003–March 2008 were computed. The autocorrelation functions for these data for all 50 m towers are shown in Figure 9. The presence of a deterministic component with a period of about one year is clearly visible

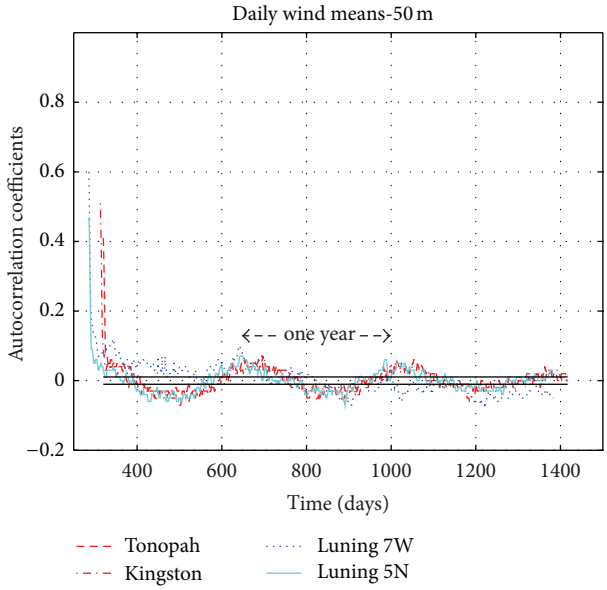

Figure 9: Autocorrelation of the daily mean, using the 2003–2008 composite datasets, for all 50 m Towers, and at 50 m level, with 95% confidence intervals, is shown on the graph.

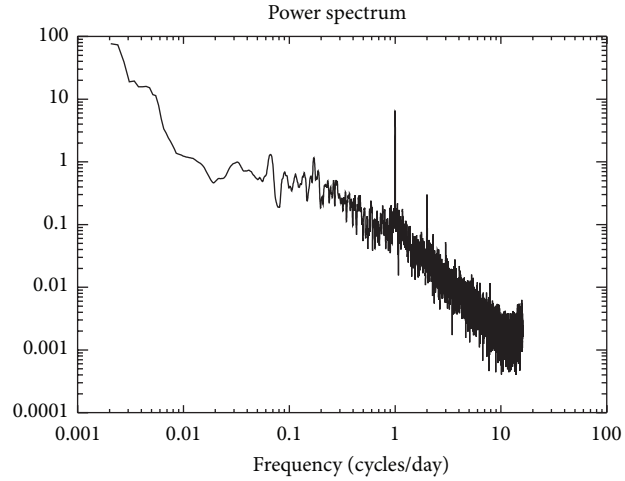

Figure 10: Power density spectra of wind speed variations with time scales smaller than 1 week, the Kingston 14W Tower.

in these diagrams. Once again this is in very good agreement with the periodicity found in Figures 5 and 6 of the moving average wind speed diagrams.

4. Spectral Analysis of the Wind Speed

We decided to compute the power spectra by the standard and well-proven method of Blackman and Tukey [28]. This is a two-stage method in which the autocorrelation is first calculated from the data and is then transformed and smoothed to obtain the power spectrum. An analysis of the wind variations for time scales, ranging from one week to one month, does not evidence any specific seasonality or periodicity. Considering a random variable in the time domain $x = x(t)$, the complex Fourier components in the frequency domain are computed considering a finite time factor by

$$X(f,T) = \int_0^T x(t) \cdot \exp(2\pi f t i)\, dt, \tag{10}$$

where x is a random variable in the time domain, t is the elapsed time, f is the frequency, X is the complex Fourier components in the frequency domain, i is the complex number unity, and T is the finite time sequence. The transformed component X is now a function not only of frequency but also of the finite time length. For small time periods, (10) cannot be satisfied due to lack of statistical significance and due to ignoring the effects of related physical properties associated with wind speed fluctuations. Power density spectra of wind speed time series with time scales lower than one week for all 50 m towers are showing a distinct peak with a period of one day, as the one shown in Figure 10 for the Kingston 14SW Tower. This is in full agreement with the periodicities found in the autocorrelations of the wind speed and direction.

4.1. The Macrometeorological Spectrum. Following the approach of Harris [29], we decided to compute the spectra of the autocorrelation functions by using the two-stage method. First, we compute the autocorrelation functions from the 10-minute and hourly data, using the 2003–2008 composite datasets, and use the Fourier transformation and smoothing to obtain the spectra. There are several reasons for this choice such as the following: (i) the effects of various non-stationarities, offsets, and the various choices of the smoothing on the result of the calculation are well documented; (ii) the availability of the autocorrelation for inspection as an intermediate product is a distinct advantage, especially when the existence of deterministic period components is suspected; and (iii) the principal disadvantage of the methods compared with the FFT algorithm, the larger computer time required, is not essential since PC time is free. Given the autocorrelation functions, it is possible to compute the normalized power spectrum for these functions numerically:

$$\int_0^\infty R(\tau) \cos(2\pi n \tau)\, d\tau = \frac{S(n)}{\sigma^2}. \tag{11}$$

Here, $R(\tau)$ is the autocorrelation coefficient at lag τ, σ is the standard deviation, $S(n)$ is the power spectrum, and n is the frequency. Hanning smoothing was applied to the Blackman and Tukey algorithm. The results are shown in Figure 11 for the Kingston 14SW composite dataset. The macro-meteorological spectra obtained are very similar to the ones found in the literature [19, 26]. These spectra are showing a very strong diurnal component, in a very good agreement with our findings in the previous analyses. This is a very important result for wind energy system operation, management, and grid integration.

5. Concluding Remarks

The annual mean wind speeds for the four towers' wind observations at 50 m height were calculated as 5.49 m/s

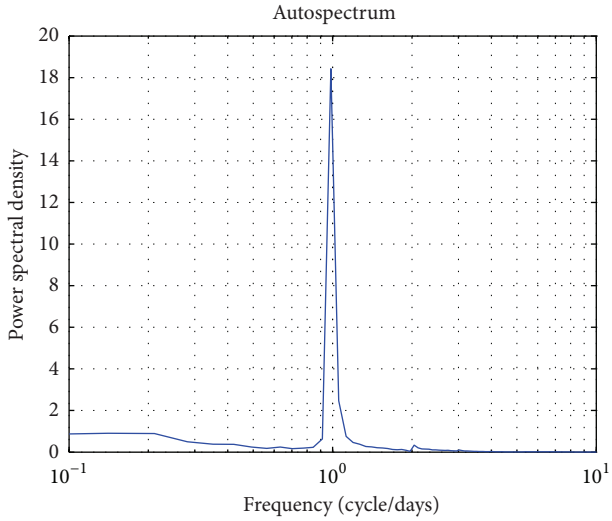

Figure 11: Macrometeorological spectrum of the Tonopah 24NW, 50 m level dataset.

(Tonopah 24NW), 4.53 m/s (Kingston 14SW), 3.96 m/s (Luning 7W) and 3.81 m/s (Luning 5N). For the Stone Cabin Tower at the 60 m level, this value was found to be 5.68 m/s. The observed data show that the maximum seasonal wind speeds for all sites are during spring. The highest potential in terms of wind energy was estimated at the Tonopah 24NW and the Stone Cabin sites, with mean wind speeds above 5.5 m/s during the peak period of every year. The same pattern of the monthly mean wind speeds was found at all other towers, but with lower values, being less suited for wind energy generation. The fitted Weibull and von Mises distributions for the observed wind speed and wind direction datasets at all towers and heights are in very good agreement with the observed wind speed distributions.

The analysis of the wind speed variations at each of the instrumented towers in Western Nevada shows the following: (i) there is a strong coherence between wind speed and direction; (ii) for time scales smaller than 24 hours, the wind speed is statistically independent, thus indicating the possibility of smoothing the total available wind power for small time scales; (iii), there is a strong diurnal periodicity in the wind speed signals, for all towers and all heights, with a maximum during the late afternoon, as found in the power spectra and diurnal variations of the wind speeds, almost coincidental with the daily peak-load demand [25]; (iv) for scales larger than 24 hours, the wind speed coefficients (mean wind speed, mean wind direction, and turbulence intensity) for each site are rather the same and are quasi-synchronized; and (v) there are strong annual oscillations in the wind speeds, with a maximum during spring and with the minimum during fall, for all towers and all heights of observation. To complete the analysis for these small wind speed time-scale variations, a higher frequency of wind velocity measurements is needed. The spectral analysis further confirms the existence of characteristic diurnal and annual time periods in the wind speeds.

Although the mean wind speeds show differences due to specifics of the measurement location, the coefficients of variation of the turbulence intensity are quite similar for all five sites. This confirms that the regional synoptic processes are dominant for the variability of the wind speed on the scale of the tower locations within a domain ranging more than $200 \times 200\,\text{km}^2$. This is further supported by the noticeably high correlation coefficients of about 0.6 between the towers for small time lags. Additional analyses, such as the distance dependence of the correlation coefficients, copulas, bootstrapping, or long-time variability of the correlations, are planned in a future study with the inclusion of additional data (in the process of analysis) collected at the other four towers in Nevada operated between 2006 and 2011.

Acknowledgments

One of the authors (D. Koracin) acknowledges support from the DOE-NREL, Grant no. NDO 5-4431-01. The authors are grateful to Greg McCurdy for assistance in obtaining data and to Travis McCord for editorial assistance.

References

[1] D. Koracin, R. G. Belu, K. Horvath, B. Candillas, and J. Jiang, "A review of challenges in assessment and forecasting of wind energy resources," *Croatian Meteorological Journal*. In press.

[2] R. Belu and D. Koracin, "Wind characteristics and wind energy potential in western Nevada," *Renewable Energy*, vol. 34, no. 10, pp. 2246–2251, 2009.

[3] K. Klink, "Climatological mean and interannual variance of United States surface wind speed, direction and velocity," *International Journal of Climatology*, vol. 19, pp. 471–488, 1999.

[4] M. J. M. Stevens and P. T. Smulders, "The estimation of parameters of the Weibull wind speed distribution for wind energy utilization purposes," *Wind Engineering*, vol. 3, no. 2, pp. 132–145, 1979.

[5] H. Basumatary, E. Sreevalsan, and K. K. Sasi, "Weibull parameter estimation—a comparison of different methods," *Wind Engineering*, vol. 29, no. 3, pp. 309–316, 2005.

[6] C. L. Archer and M. Z. Jacobson, "Spatial and temporal distributions of US winds and wind power at 80 m derived from measurements," *Journal of Geophysical Research D*, vol. 108, no. 9d, 2004.

[7] A. H. Monahan, "The probability distribution of sea surface wind speeds. Part I: theory and SeaWinds observations," *Journal of Climate*, vol. 19, no. 4, pp. 497–520, 2006.

[8] R. D. Christofferson and D. A. Gillete, "A simple estimator of the shape factor of the two-parameter Weibull distribution," *Journal of Climate and Applied Meteorology*, vol. 26, pp. 323–325, 1987.

[9] D. M. Deaves and I. G. Lines, "On the fitting of low mean windspeed data to the Weibull distribution," *Journal of Wind Engineering and Industrial Aerodynamics*, vol. 66, no. 3, pp. 169–178, 1997.

[10] K. Conradsen, L. B. Nielsen, and L. P. Prahm, "Review of Weibull statistics for estimation of wind speed distributions," *Journal of Climate & Applied Meteorology*, vol. 23, no. 8, pp. 1173–1183, 1984.

[11] J. V. Seguro and T. W. Lambert, "Modern estimation of the parameters of the Weibull wind speed distribution for wind

energy analysis," *Journal of Wind Engineering and Industrial Aerodynamics*, vol. 85, no. 1, pp. 75–84, 2000.

[12] D. Weisser and T. J. Foxon, "Implications of seasonal and diurnal variations of wind velocity for power output estimation of a turbine: a case study of Grenada," *International Journal of Energy Research*, vol. 27, no. 13, pp. 1165–1179, 2003.

[13] M. Martín, L. V. Cremades, and J. M. Santabàrbara, "Analysis and modelling of time series of surface wind speed and direction," *International Journal of Climatology*, vol. 19, no. 2, pp. 197–209, 1999.

[14] T. P. Chang, "Estimation of wind energy potential using different probability density functions," *Applied Energy*, vol. 88, no. 5, pp. 1848–1856, 2011.

[15] J. C. Chadee and C. Sharma, "Wind speed distributions: a new catalogue of defined models," *Wind Engineering*, vol. 25, no. 6, pp. 319–337, 2001.

[16] T. P. Chang, "Performance comparison of six numerical methods in estimating Weibull parameters for wind energy application," *Applied Energy*, vol. 88, no. 1, pp. 272–282, 2011.

[17] J. A. Carta, C. Bueno, and P. Ramírez, "Statistical modelling of directional wind speeds using mixtures of von Mises distributions: case study," *Energy Conversion and Management*, vol. 49, no. 5, pp. 897–907, 2008.

[18] J. A. Carta, P. Ramírez, and S. Velázquez, "A review of wind speed probability distributions used in wind energy analysis. Case studies in the Canary Islands," *Renewable and Sustainable Energy Reviews*, vol. 13, no. 5, pp. 933–955, 2009.

[19] O. E. Smith, Vector wind and vector shear models 0 to 27 km altitude at Cape Kennedy, Florida and Vandenberg AFB, California, NASA-TM-X-73319h.

[20] J. A. Carta and P. Ramírez, "Analysis of two-component mixture Weibull statistics for estimation of wind speed distributions," *Renewable Energy*, vol. 32, no. 3, pp. 518–531, 2007.

[21] D. Koracin, R. Reinhardt, G. McCurdy et al., "Wind energy assessment study for nevada—tall tower deployment (Stone Cabin)," Tech. Rep. NREL/SR-550-47085, DOE-NREL, 2009, http://www.nrel.gov/docs/fy10osti/47085.pdf.

[22] R. G. Belu and D. Koracin, "Effects of complex wind regimes and meteorological parameters on wind turbine performances," in *Proceedings of the IEEE Energy Tech*, CD Proceedings, Cleveland, Ohio, USA, May 2012.

[23] J. Q. Stewart, C. D. Whiteman, W. J. Steenburgh, and X. Bian, "A climatological study of thermally driven wind systems of the U.S. Intermountain West," *Bulletin of the American Meteorological Society*, vol. 83, no. 5, pp. 699–708, 2002.

[24] M. E. Jeglum, W. J. Steenburgh, T. P. Lee, and L. F. Bosart, "Multi-reanalysis climatology of intermountain cyclones," *Monthly Weather Review*, vol. 138, no. 11, pp. 4035–4053, 2010.

[25] J. Manwell, J. McGowan, and A. Rogers, *Wind Energy Explained: Theory, Design and Application*, John Wiley & Sons, New York, NY, USA, 2002.

[26] H.-C. Lim and T.-Y. Jeong, "Wind energy estimation of the Wol-Ryong coastal region," *Energy*, vol. 35, no. 12, pp. 4700–4709, 2010.

[27] G. McLachlan and D. Peel, *Finite Mixture Models*, John Wiley & Sons, New York, NY, USA, 1st edition, 2000.

[28] R. B. Blackman and J. W. Tukey, *The Measurement of Power Spectrum From the Point of View of Communications Engineering*, Dover, New York, NY, USA, 1959.

[29] R. I. Harris, "The macrometerological spectrum—a preliminary study," *Journal of Wind Engineering and Industrial Applications*, vol. 96, pp. 2294–2307, 2008.